

# Synthesis of New Derivatives of Boehmeriasin A and their Biological Evaluation in Liver Cancer

*Ece Akhan Güzelcan,<sup>a</sup> Marcus Baumann,<sup>b,c,\*</sup> Ian R. Baxendale,<sup>b</sup> Rengul Cetin-Atalay,<sup>a,\*</sup>*

<sup>a</sup> Graduate School of Informatics, Cancer Systems Biology Laboratory, METU, 06800 Ankara,  
Turkey

<sup>b</sup> Department of Chemistry, University of Durham, South Road, DH1 3LE, Durham, UK

<sup>c</sup> School of Chemistry, University College Dublin, Science Centre South, Belfield, Dublin 4,  
Ireland

**Key words:** boehmeriasin A, natural product analogs, liver cancer, cell cycle analysis

## ABSTRACT

Primary liver cancer is the sixth most frequent and the second most deadly cancer worldwide and the global epidemic of non-alcoholic fatty liver disease is expected to severely impact on the epidemiology of this cancer. Due to the limited availability of effective chemotherapeutic agents, novel bioactive molecules are urgently required. To address this, two series of boehmeriasin A analogs have been synthesized in short and high yielding processes providing derivatives differing either in the alkaloid's pentacyclic scaffold or its peripheral substitution pattern. These series have enabled, for the first time, comparative studies into key biological properties revealing a new lead compound with exceptionally high activity against liver cancer cell lines in the picomolar range for both well (Huh7, Hep3B and HepG2) and poorly (Mahlavu, FOCUS and SNU475) differentiated cells. The cell death, induced by the compounds **1** and **19**, was characterized as apoptosis by cytochrome-C release, PARP protein cleavage and SubG1 cell cycle arrest. Subsequent testing associated apoptosis via oxidative stress with in situ formation of ROS and altered phospho-protein levels. Compound **19** decreased Akt protein phosphorylation which is crucially involved in liver cancer tumorigenesis. Given its simple synthetic accessibility and the intriguing biological properties of our new lead compound this has unique potential to address unmet challenges within liver cancer therapy.

## Introduction

Primary liver cancer (hepatocellular carcinoma, HCC), is the sixth most frequent cancer type and the second highest cause of cancer-related death worldwide [1]. Viral infections with hepatitis B or C, alcoholic injury, obesity and other factors inducing cirrhosis and chronic liver disease are the major risk factors for HCC [2-4]. It is also expected that the rate of liver cancer and associated deaths will increase in the coming years due to the global epidemic of non-alcoholic fatty liver disease (NAFLD) [5]. Despite the well-known etiological factors, liver cancer remains one of the most lethal types of cancer, due to very limited therapeutic options with significant clinical benefits [6]. Liver resection, transplantation and chemoembolization are still the most amenable options to remedy, however, not all the patients meet the criteria for these treatments [7]. Meanwhile, patients with advanced HCC suffer from the lack of effective therapy. The first FDA approved drug Sorafenib (**5**, Figure 1), which is a multi-kinase inhibitor, can only improve patients' median survival for about 3 months [8]. Very recently the closely related multi-kinase inhibitor Regorafenib was used in patients as a second line treatment. The mean survival was about 10 months compared to a placebo (~8 months) [9].

To address these challenges in the arena of liver cancer [10], we decided to investigate the chemical synthesis and biological evaluation of new analogs of the known plant alkaloid boehmeriasin A.

Boehmeriasin A (**1**, Figure 1) is a pentacyclic phenanthroquinolizidine alkaloid recently isolated from the ethanolic extract of *boehmeria siamensis* Craib [11], a plant that has long been used in south-east Asia for the treatment of rheumatism as well as skin diseases such as urticaria (hives). Upon extensive biological studies, it was revealed that **1** possesses significant activity

against several cancer cell lines commonly exceeding the potency of Taxol by at least tenfold. The nanomolar cytotoxic activity of boehmeriasin A was established for various cancer cells, originating from lung, colon, breast, prostate, kidney cancers, and leukemia [12]. In addition to this anti-cancer activity boehmeriasin A also causes G1 cell cycle arrest, cellular differentiation, affects cellular morphology and results in lipid droplet accumulation in breast cancer cells [13]. It was furthermore found that boehmeriasin A shares this promising anti-cancer activity with other members of the phenanthroquinolizidine and -pyrrolizidine alkaloids such as tylophorine (2), antofine (3) and cryptopleurine (4) (Figure 1) [14-21].

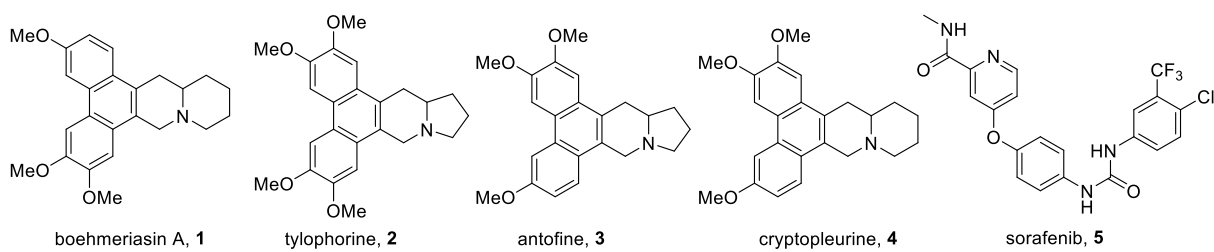


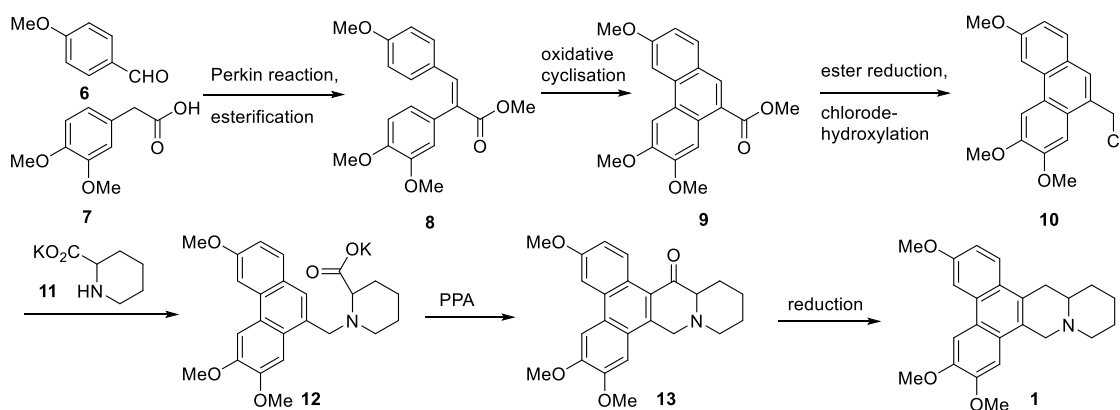
**Figure 1:** Structures of racemic boehmeriasin A **1**, related alkaloids (**2-4**) and sorafenib (70%).

Driven by the promising bioactivity reports, many successful total syntheses of these intriguing cytotoxic alkaloids have been disclosed [12,22-24]. Despite these efforts neither the molecular target nor the mode of action of these important structures have been identified and detailed SAR studies are lacking, which does severely hamper further progress in the development towards boehmeriasin A based drug leads. To establish this missing key data, we wished to evaluate boehmeriasin A as well as several new analogs in the context of human epithelial cancers especially in liver cancer.

**Analog Synthesis:** Upon analysis of the parent pentacyclic scaffold of boehmeriasin A (**1**) and its closely related natural products (**2-4**) we decided to design and synthesize two series of target

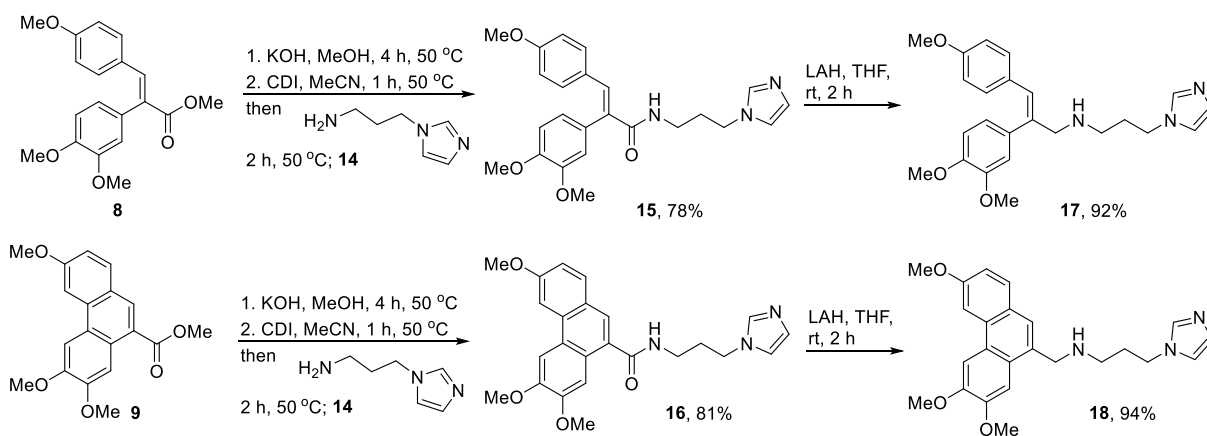
compounds to study structure-activity relationships of these entities. Thus, a first series would retain the oxygenation pattern of boehmeriasin A but introduce alterations in the connectivity of the fused ring system, whereas in a second series the pentacyclic framework would be conserved while modifications to the embedded quinolizidine system would be made.

To create these two series, we decided to exploit a synthetic route to boehmeriasin A itself which we had developed previously (Scheme 1) [24]. This route is based on an efficient 7-step sequence in which a Perkin reaction is followed by an esterification to yield building block **8** that was then converted into the phenanthrene unit **9** by a FeCl<sub>3</sub>-mediated oxidation. The pendant ester functionality was reduced to an alcohol and activated as a chloride (**10**) to then allow coupling with pipecholic acid (**11**). Subsequent treatment of **12** with polyphosphoric acid (PPA) led to ring closure via a Friedel-Crafts acylation reaction and furnished ketone **13** that upon full reduction rendered the desired natural product **1**. This approach was deemed very attractive as it is robust and scalable and furthermore allows to introduce desirable variations on different moieties of the parent structure of **1**.



**Scheme 1:** Previous synthesis of racemic boehmeriasin A (**1**).

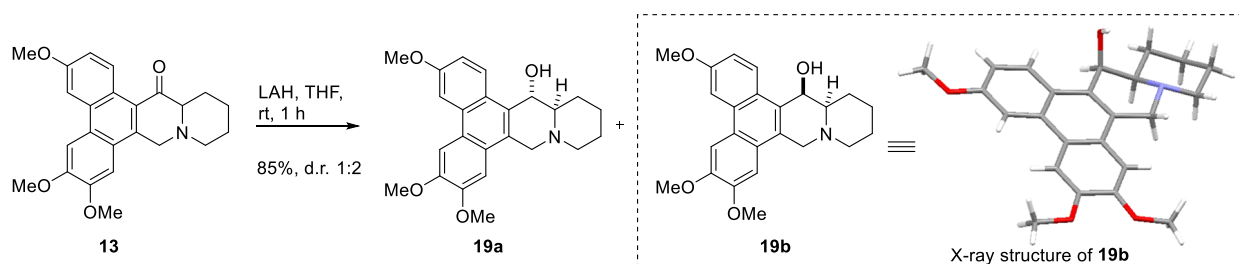
The synthesis of the first series of analogs made use of intermediates **8** and **9** that were independently elaborated by amide coupling with aminopropyl imidazole (**14**, Scheme 2), which was chosen as a hydrophylic appendage to mimic the quinolizidine substructure of **1** and at the same time improve the bioavailability of these species. Furthermore, it was intended to modulate the planarity of the phenanthrene system by omitting the central C-C bond in some of the analogs, which would enable us to evaluate the likelihood of these entities to act via DNA interchelation.



**Scheme 2:** Synthesis of analogs **15-18** (Series 1).

To this end both **8** and **9** were hydrolyzed under basic conditions rendering the corresponding carboxylic acid derivatives, that were subsequently activated by CDI and coupled with aminopropyl imidazole (**14**) to furnish the desired amides **15** and **16** in good yield. In addition, both amides were treated with LAH (2.5 equiv.) to obtain the corresponding amines **17** and **18** allowing to establish the effect of having an amide versus an amine incorporated into these structures, which could have implications due to altered H-bonding patterns.

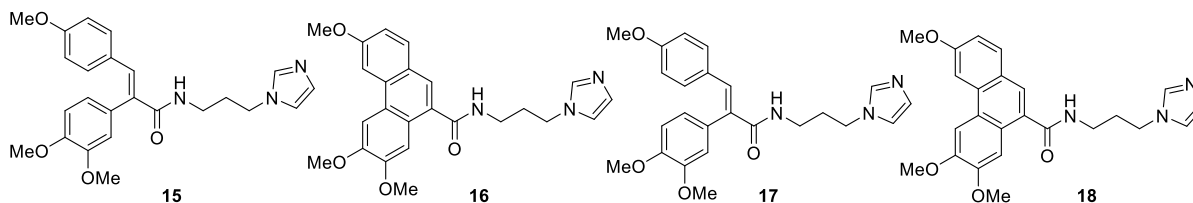
With selected examples of a first analog series in hand we turned our attention to a second series in which we envisaged to study alterations on the pentacyclic framework of boehmeriasin A. Specifically, we decided to explore manipulations on the carbonyl of **13** by means of its reduction to the corresponding alcohol derivatives. The synthesis of the desired alcohols was readily accomplished by reduction of **13** by LAH (2.0 equiv.) giving a mixture of diastereomeric alcohol products **19a** and **19b** in a 1:2 ratio. Pleasingly, as it was possible to separate this mixture by preparative TLC we were able to undertake characterization and subsequent biological evaluation of the individual diastereomers. Additionally, single crystal X-ray diffraction experiments were used to identify the major diastereomer **19b** as the *trans*-alcohol product (Scheme 3).



**Scheme 3:** Synthesis of analogs **19a** and **19b** from ketone **13** (Series 2).

Together with boehmeriasin A (**1**) and its carbonyl derivative **13**, these individual alcohol derivatives **19a** and **19b** therefore represent the second series of analogs available for detailed biological testing (Figure 2).

#### Analog series 1:



#### Analog series 2:

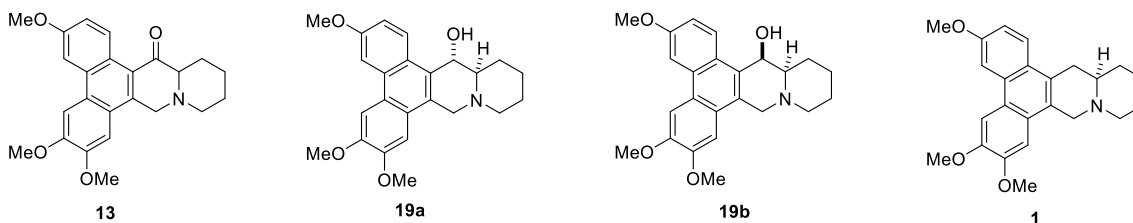


**Figure 2:** Overview of both series of new boehmeriasin A analogs.

### Biological Studies:

#### 2.1 Biological Activities of First Series of Boehmeriasin A Analogs

Commencing our studies with boehmeriasin A analogs **15-18** we analyzed their cellular toxicity against different hepatocellular carcinoma cells, namely Huh7 and Mahlavu. As pointed out earlier we wished to establish whether simplified structures possessing a conformationally open ring system would still impart significant cytotoxicity, whilst improving solubility by introduction of an imidazole appendage. However, to our surprise it was found that these analogs displayed either very moderate activity (compounds **16** and **17**  $IC_{50}$  10-54  $\mu$ M) or no activity (compounds **15** and **18**, Table 1). Additionally, the presence of an amide or amine linkage as well as the central biaryl bond appears to be irrelevant for any activity against these cell lines. Whilst somewhat unexpected this finding establishes clearly that the pentacyclic framework of the boehmeriasins is crucial for their sub-micromolar biological activity which had not been

demonstrated before. This furthermore highlights the importance of the embedded quinolizidine substructure and prompted us to evaluate analogs of our second series next.

**Table 1:** Cytotoxicity of compounds **15-18** evaluated in HCC cells.

Compound	IC <sub>50</sub> Values (μM)	
	Huh7	Mahlavu
<b>15</b>	NI	NI
<b>16</b>	19.2	54
<b>17</b>	9.3	13.8
<b>18</b>	NI	NI

\*NI: No inhibition

## 2.2 Cytotoxicity of Second Series of Boehmeriasin A Derivatives

To verify the anticipated biological activity of the parent boehmeriasin A (**1**) and its analogs (**12**, **13**, **19**) an initial screen against different epithelial cancer cells, namely liver (Huh7), breast (MCF7) and colon (HCT116) carcinoma cells was performed. The cytotoxicity of each compound was assessed by sulforhodamine B (SRB) assay. IC<sub>50</sub> values of the synthesized compounds were calculated for each cell line following 72 hours of treatment (Table 2).

**Table 2:** Initial screening of compounds **1**, **12**, **13** and **19**.

Compound	IC <sub>50</sub> Values (μM)		
	Huh7	MCF7	HCT116
<b>1</b>	0.008	0.005	0.7
<b>19</b>	0.002	0.001	< 0.001
<b>12</b>	NI	NI	NI
<b>13</b>	12	7	8.1

\*NI: No inhibition

In general, boehmeriasin A (**1**) and its hydroxy analog **19** (as 1:2 mixture of diastereomers) were identified as promising anti-cancer compounds due to their low nanomolar IC<sub>50</sub> values. Although ketone derivative **13** showed moderate cytotoxicity, when compared to **1** and **19** its bioactivity was low despite the only minor alteration of its structure. Additionally, the carboxylate species **12** had no cytotoxic bioactivity against these cancer cells, possibly as it does not easily permeate into cells due to its nature being a salt. Furthermore, this result is in line with the loss of activity seen for the other ‘open-structured’ analogues **15-18**.

Considering the lack of HCC targeted chemotherapeutic agents and based on our specific aim in this study, we furthermore tested these compounds (**1**, **12**, **13** and **19**) against various liver cancer cell lines. Therefore, we assessed the IC<sub>50</sub> values of these compounds in a HCC cell panel (Huh7, Mahlavu, SNU475, FOCUS, Hep3B and HepG2) (Table 3).

**Table 3:** Cytotoxicity of compounds in HCC cell panel.

<b>IC<sub>50</sub> Values (μM)</b>						
<b>Compound</b>	<b>Huh7</b>	<b>Hep3B</b>	<b>HepG2</b>	<b>Mahlavu</b>	<b>SNU475</b>	<b>FOCUS</b>
<b>1</b>	0.008	0.016	0.06	0.016	0.014	0.02
<b>19</b>	0.002	0.017	2.7 ± 0.9	0.01	0.015	0.012
<b>12</b>	NI	NI	NI	NI	NI	NI
<b>13</b>	12	45	NI	35	19.1	5

\*NI: No inhibition

Similarly to our results presented in Table 2, compounds **1** and **19** were found to be significantly cytotoxic in all cell types of HCCs. Crucially, **1** and **19** displayed nanomolar IC<sub>50</sub> values not only for well differentiated HCC cells such as Huh7, Hep3B and HepG2 but also for poorly differentiated and more aggressive cells which are Mahlavu, FOCUS and SNU475. Therefore, **1**

and **19** can be considered potential anti-cancer drug candidates in liver cancer cells. On the other hand, **13** displayed limited cytotoxic activity and **12** had no activity in any type of HCC cells.

### 2.3. Real-time assessment of hepatocellular carcinoma cell growth upon treatment with compounds **1** and **19**

A real-time cell electronic sensing (RT-CES) assay was used to evaluate the bioactivities of boehmeriasin A and its analogs on well differentiated Huh7 cells and poorly differentiated Mahlavu cells. According to the data obtained from RT-CES, the time dependent IC<sub>50</sub> values were calculated (Table 4). In general, the RT-CES results support the findings of the above SRB assay. Candidates **1** and **19** caused severe growth inhibition in both Huh7 and Mahlavu cells (Figure 3). The real-time growth inhibition pattern suggested a cell cycle arrest in cells treated with **1** and **19**, as DMSO treated cells retain their proliferation profile until they become confluent (2).

**Table 4:** Time dependent IC<sub>50</sub> values of compounds **1** and **19**.

Compound	IC <sub>50</sub> Values (μM)					
	Huh7			Mahlavu		
	24 h	48 h	72 h	24 h	48 h	72 h
<b>1</b>	2 μM	1 μM	0.8 μM	0.6 μM	0.5 μM	0.6 μM
<b>19</b>	1.9 μM	0.8 μM	0.6 μM	0.4 μM	0.1 μM	0.1 μM

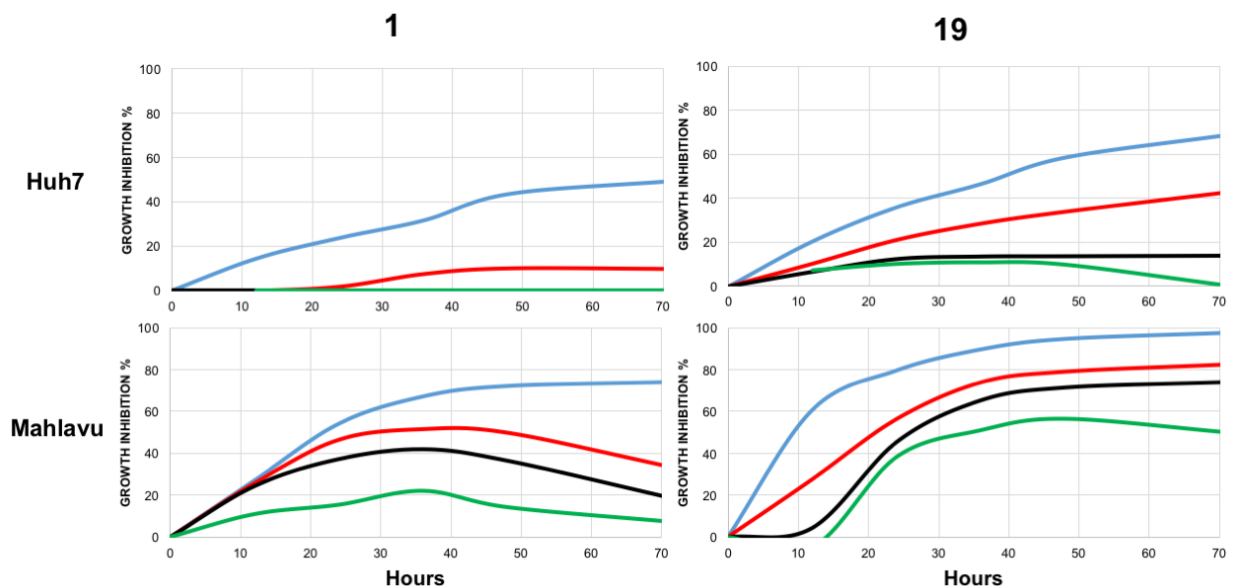


**Figure 3:** Real-time cellular proliferation assay. RT-CES analysis of Huh7 and Mahlavu cell lines treated with various concentrations of the compounds **1** and **19**. Blue: 1  $\mu\text{M}$ , Red: 0.5  $\mu\text{M}$ , Black: 0.25  $\mu\text{M}$ , Green: 0.125  $\mu\text{M}$ . DMSO is used as solvent control and percent cell growth data is normalized according to DMSO controls.

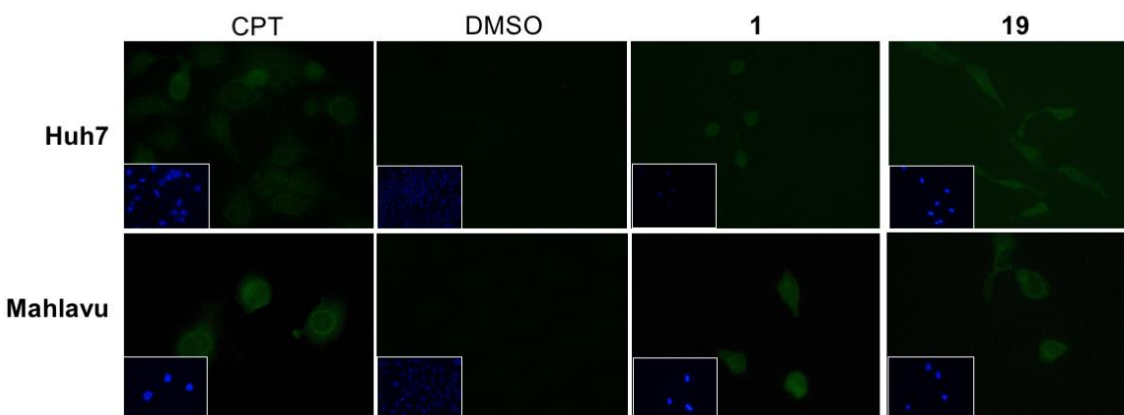
The curvature of our real time cell death data and the measured  $\text{IC}_{50}$  values imply that the cell death associated with these compounds could be apoptosis. The differences of  $\text{IC}_{50}$  values between SRB end point colorimetric assay and the RT-CES can be due to the evaluation of distinct cellular elements. While SRB detects the total protein levels, RT-CES is dependent on the cell surface attachment. During apoptosis there is a high destruction of cellular proteins which leads to less colorimetric data collection. Therefore, it is common to observe  $\text{IC}_{50}$  differences between cell death detection techniques. Hence in this study, we established the bioactivities of the new boehmeriasin A analogs with two complementary techniques.

## 2.4. Characterization of Cell Death Mechanism Induced by Boehmeriasin Derivatives

The cell death mechanism of the cells treated with boehmeriasin A or its derivatives was initially analyzed by observing the release of cytochrome-C which was examined via fluorescence microscopy (Figure 4A). Camptothecin (CPT) was used as positive control for cytochrome-C release, showing that cytochrome-C levels in cells treated with **1** and **19** were comparable to the positive control. A significant increase in the release of cytochrome-C in cells treated with **1** and **19** indicates apoptotic cell death.

The activation of apoptotic pathways by boehmeriasin A derivatives was further studied by evaluating the status of one the most well-known apoptotic proteins, PARP. Here a significant increase in PARP cleavage in the cells treated with **19** was identified and did become significant within 72 h in cells. Compared to boehmeriasin A itself, its hydroxy-derivative **19** displayed a more significant effect on PARP cleavage that is paralleled by its increased cytotoxic effect on liver cancer cells (Figure 4B).

**A**



## B

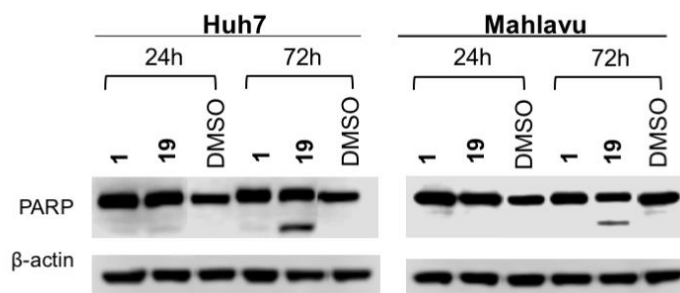


**Figure 4:** Analysis of apoptotic processes in cells treated with Boehmeriasin A derivatives. (A) The evaluation of Cytochrome C release in Huh7 and Mahlavu cells treated with 1  $\mu$ M **1** and **19**. (B) PARP cleavage in Huh7 and Mahlavu cells treated with 1  $\mu$ M **1** and **19** for 24 and 72 hours. DMSO is used as solvent control.

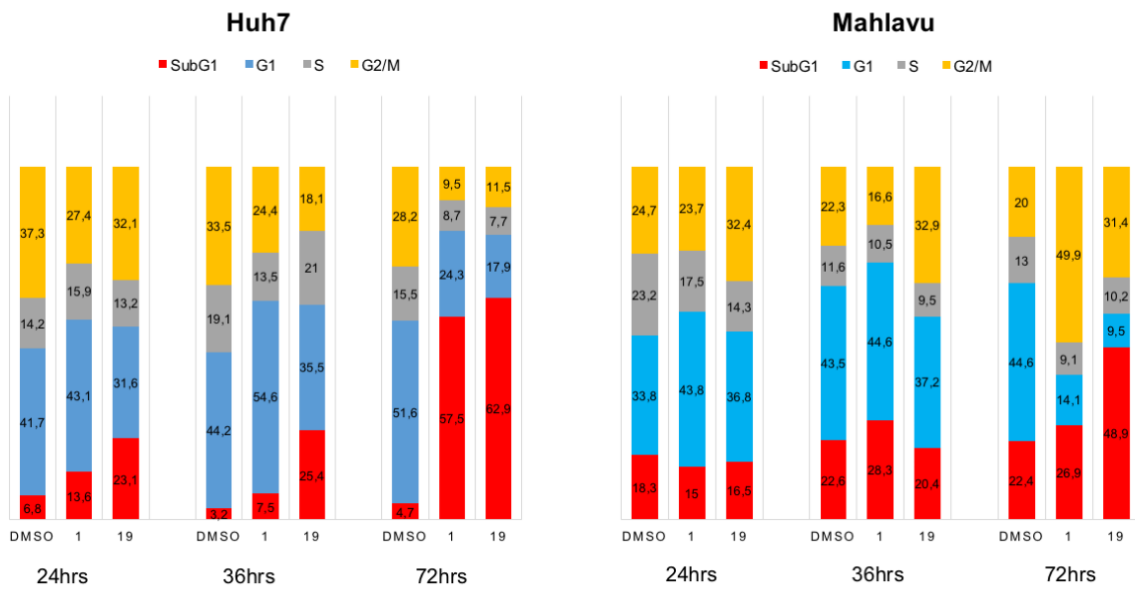
### 2.5. Cell Cycle Analysis of HCC Cells treated with Boehmeriasin Derivatives

To identify the effect of boehmeriasin derivatives on the cell cycle progress flow cytometry analysis was performed using propidium iodide (PI) staining in Huh7 and Mahlavu liver cancer cells. Upon treatment with **1** and **19**, increasing levels of apoptotic cells along with SubG1 arrest were observed. The most significant increase was observed at 72 h. **19** resulted in the higher number of cells that accumulated at SubG1 phase. Additionally, HCC cells treated with **1** also led to an increase in SubG1, however this effect became more notable after 72 h (Figure 5 A, B). In addition, the effect of boehmeriasin A derivatives on the cell cycle was further investigated in Huh7 and Mahlavu cell by western blot analysis of the proteins which are involved in this process. **1** and **19** down-regulated Cyclin B1 (CDK1 regulator and mitotic initiator in the late G2 phase) and its companion CDK1 (essential for G1/S and G2/M phase transitions) levels in Huh7

cells. Treatment with **1** and **19** also reduced the CDK2 (G1 to S phase transition) and its regulator Cyclin E level, which became more significant at 72h. Altogether, these results indicate that boehmeriasin A derivatives induce cell cycle arrest at G2/M and SubG1 phases which is followed by apoptosis in these cells (Figure 5A).

The effect of these compounds on cell cycle protein expression is more pronounced on Huh7 cells (Figure 5B). Mahlavu cells are reported as more resistant to small molecule inhibitors due to PTEN deletion in PI3K/Akt signaling pathway [25]. The effect of the compounds can still be observed even in these cells. Furthermore, the active phosphorylated form of Akt protein is significantly down-regulated with compound 19 at 72 hours (Figure 5B).

**A**



**B**

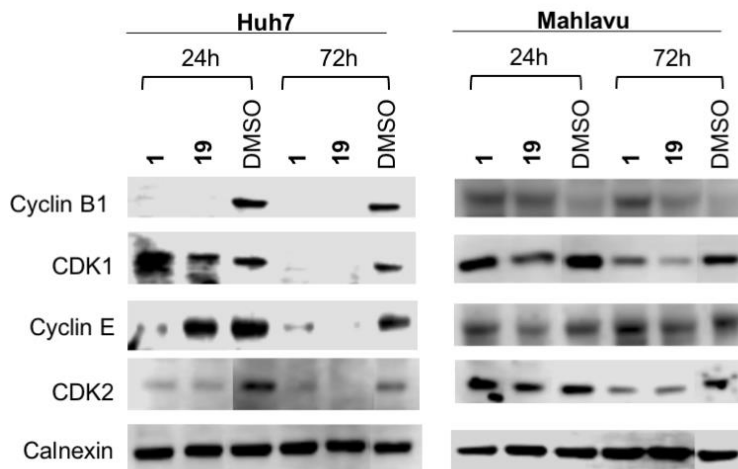


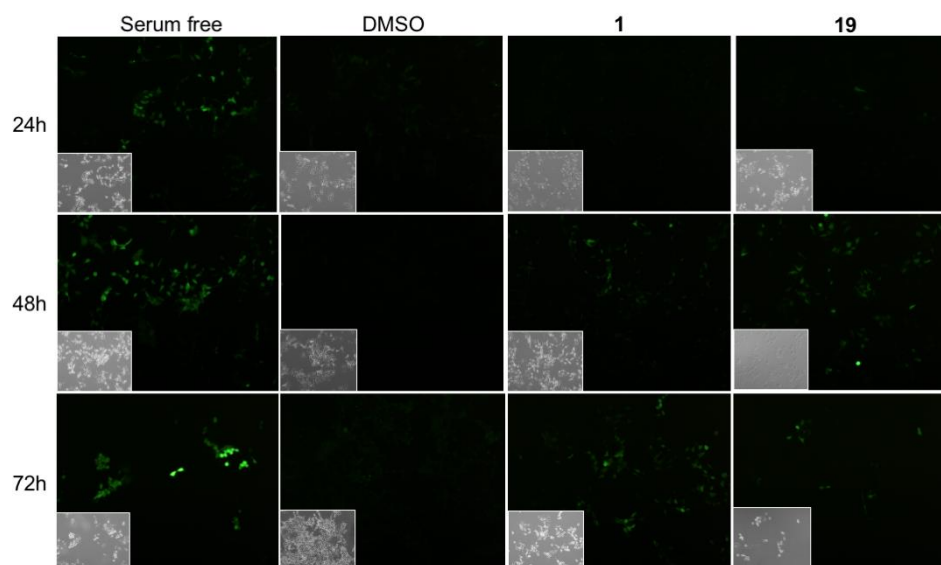
**Figure 5:** The assessment of the cell cycle status of cells treated with boehmeriasin A derivatives (A) The time dependent cell cycle analysis of treated Huh7 and Mahlavu cells with flow cytometry (B) Comparative analysis cell cycle protein expression in the presence of **1** and **19**. DMSO is used as solvent control.

## 2.6. Release of Reactive Oxygen Species and Stress Mechanism Induced by Boehmeriasin Derivatives

Reactive oxygen species (ROS), depending on their dose, can alter cellular pathways and promote cell cycle arrest and apoptosis in liver cancer cells [25]. The released ROS can be visualized using the 2,7-dichlorofluorescein diacetate (DCFH-DA) assay. The presence of fluorescence stain, which is detected via fluorescence microscopy, indicates ROS activity and thus cellular stress. Evaluating the presence of ROS in liver cancer cells that were treated with boehmeriasin A and its derivatives showed that the ROS activity in cells treated with **1** and **19** was significantly increased and became comparable to the positive control. The ROS activity increased with time of incubation of **1** and **19** (Figure 6A).

In addition, as boehmeriasin analogs induced oxidative stress, these were assessed by evaluating the phosphorylation status of the proteins involved in the ROS pathway via western blot [5]. It was found that both Mahlavu and Huh7 cells treated with **1** and **19** led to a decrease of the phosphorylated Ser-966-ASK1 levels which is associated with cellular oxidative stress, though the effect on Mahlavu is being more prominent [5] (Figure 6B). Mahlavu cells are characterized by a hyperactive PI3K/AKT pathway due to PTEN protein deletion and therefore we observe differential downstream P-SAPK/JNK protein levels. The stress protein SAPK/JNK phosphorylation was increased in Huh7 cells treated with both **1** and **19**. In Mahlavu cells the P-SAPK/JNK levels were differentially altered with **1** and **19** treatments in parallel to AKT phosphorylation status. The compound **19** decreases the p-AKT levels which is the active form of this protein for cell survival. Our data indicates that the novel compound **19** gains its intriguing bioactivity through PI3K/AKT pathway modulation which is strategically involved in liver cancer tumorigenesis.

A



**B**

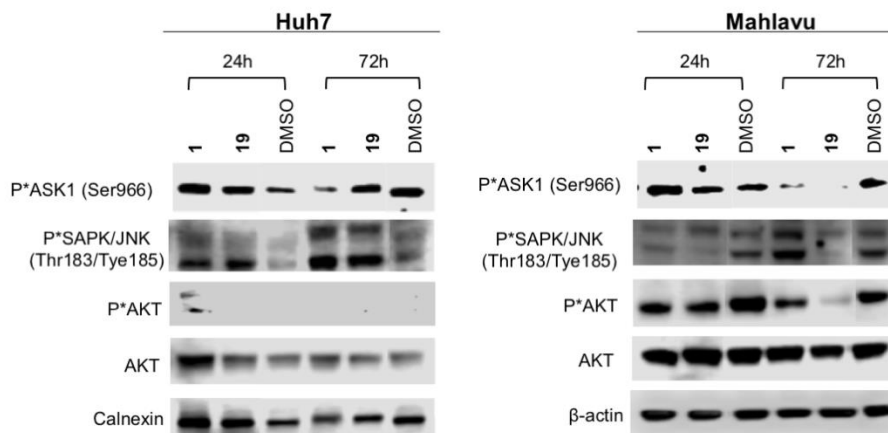


**Figure 6:** The analysis of cellular stress mechanism. (A) The evaluation of ROS activity by DCHF-DA staining in Huh7 cells treated with boehmeriasin derivatives. DCFH-DA is cell permeable dye, and, after uptake, it is cleaved by intracellular esterases to 2,7-dichlorodihydrofluorescein (DCFH<sub>2</sub>), which is trapped within the cells, and is oxidized to fluorescent 2,7-dichlorofluorescein (DCF) in the presence of ROS. The cells that grow in serum free medium were shown to induce ROS activity, therefore, we used serum free culture media as positive control. (B) The western blot analysis of the stress related proteins of boehmeriasin derivatives treated Huh7 and Mahlavu cells.

## 2.7. The bioactivity of Individual Hydroxy-Analogs 19a and 19b in HCC cells

After concluding that **19** (as a 1:2 mixture of diastereomers **19a** and **19b**) possessed the highest bioactivity, we decided to further study its individual diastereomers to establish whether a preference of the relative stereochemistry manifests in differentiated activity. The separation of this mixture of diastereomers was accomplished by preparative thin layer chromatography yielding **19a** as the minor (lower  $R_f$ ) and **19b** as the major (higher  $R_f$ ) diastereomer in a 1:2 ratio. The individual hydroxy-analogs **19a** and **19b** were initially screened in human cancer cells (Table 5) and the data was verified with SRB assays confirming not only that both hydroxy-

analogs were highly active anti-cancer compounds but moreover that **19b** displayed superior activity in the picomolar range.

**Table 5:** Cytotoxicity of compounds **19a** and **19b** evaluated in different human cancer cells.

<b>IC<sub>50</sub> Values (nM)</b>			
<b>Compound</b>	<b>Huh7</b>	<b>MCF7</b>	<b>HCT116</b>
<b>19a (minor)</b>	0.306	0.016	0.043
<b>19b (major)</b>	0.017	0.021	0.007

Correlating this intriguing finding with the single crystal X-ray structure secured for the major diastereomer **19b** (see Scheme 3) demonstrates that the highest activity results from the diastereomer having the hydroxy substituent trans to the methine proton and syn to the ring nitrogen. Although, the reason of this is not entirely clear at this point this finding might point to a specific binding mode of **19b** within its molecular target.

Despite efforts in separating the racemic **19b** by means of chiral HPLC so far having been unsuccessful, it is apparent that **19b** is a very active boehmeriasin A derivative possessing picomolar anti-cancer activity against challenging breast, colon and liver cell lines which therefore warrants further investigations. We thus believe that this opens further avenues to elucidate the specific identity and binding mode of our novel drug-lead **19b** to its molecular target.

In conclusion, we have successfully prepared two sets of new boehmeriasin A analogs featuring either a simplified structure or a complete pentacyclic framework as found in the parent alkaloid. Whilst the former was found to be significantly less active ( $IC_{50} > 10 \mu M$ ) than boehmeriasin A,

the latter series displayed superb anti-cancer activity across a range of cell lines. Minute structural changes from a ketone (**13**, H-bond acceptor) to a secondary alcohol (**19**, H-bond donor) have resulted in a 10,000-fold increase in activity, which is more pronounced in the *trans*-diastereomer (**19b**) and surpasses the activity of boehmeriasin A itself. Subsequent in-depth biological studies have revealed a broad spectrum of activities including cell cycle arrest in the sub-G1 stadium, the generation of reactive oxygen species as well as the activation of apoptotic pathways through PARP cleavage. Due to the straightforward synthetic accessibility and the intriguing biological properties of our new lead compound **19b** we foresee its potential for future developments to address unmet challenges within liver cancer therapy.

## Experimental section

### 3.1. Synthesis Procedures for New Compounds

**Rac.-Boehmeriasin A, 1** and **3,6,7-trimethoxy-12,13,14,14a-tetrahydro-9H-dibenzo[f,h]-pyrido[1,2-b]isoquinolin-15(11H)-one, 13** were prepared as reported previously [24].

**(E)-N-(3-(1H-Imidazol-1-yl)propyl)-2-(3,4-dimethoxyphenyl)-3-(4-methoxyphenyl)acrylamide, 15:** To a solution of methyl (*E*)-2-(3,4-dimethoxyphenyl)-3-(4-methoxyphenyl)acrylate (**8**, 1.0 g, 3.05 mmol) in methanol (10 mL, 0.3 M) was added an aqueous solution of KOH (5.0 M, 5 mL, 8.3 equiv. KOH). The resulting mixture was stirred at 50 °C for 4 h when tlc analysis indicated full conversion of **8**. After neutralizing with aqueous HCl (1 M) and extraction (DCM/water, 2 x 50 mL) the organic layers were combined, dried over anhydrous sodium sulfate, filtered and evaporated to dryness under reduced pressure. The solid residue was redissolved in MeCN (15 mL) and combined with carbonyldiimidazole (CDI, 500 mg, 3.09 mmol, 1 equiv.). After heating this mixture for 1 h at 50 °C aminopropylimidazole (275 mg, 3.0 mmol, 1.0 equiv.) was added and the mixture was stirred at 50 °C for a further 2 h. After evaporation of the volatiles the crude product was extracted (DCM/water, 2 x 20 mL) and isolated as an off-white solid (1.0 g, 2.4 mmol, 78 %) after drying over anhydrous sodium sulfate, filtration, evaporation and trituration from cold ethyl acetate.

**<sup>1</sup>H-NMR (400 MHz, CDCl<sub>3</sub>):** δ/ppm 7.68 (s, 1H), 7.34 (d, *J* = 1.2 Hz, 1H), 6.92 (d, *J* = 1.1 Hz, 1H), 6.91 – 6.87 (m, 3H), 6.83 (d, *J* = 1.3 Hz, 1H), 6.72 (dd, *J* = 8.2, 1.9 Hz, 1H), 6.64 (d, *J* = 1.9 Hz, 1H), 6.60 (d, *J* = 8.9 Hz, 2H), 5.73 (t, *J* = 6.1 Hz, 1H), 3.89 (t, *J* = 7.0 Hz, 2H), 3.86 (s, 3H), 3.72 (s, 3H), 3.66 (s, 3H), 3.23 (app q, *J* = 6.7 Hz, 2H), 1.90 (app p, *J* = 6.9 Hz, 2H). **<sup>13</sup>C-NMR (100 MHz, CDCl<sub>3</sub>):** δ/ppm 167.9 (C), 159.9 (C), 149.9 (C), 149.1 (C), 137.0 (CH), 136.8 (CH), 132.0 (2CH), 131.3 (C), 129.5 (CH), 128.5 (C), 127.4 (C), 122.0 (CH), 118.8 (CH), 113.7

(2CH), 112.6 (CH), 112.2 (CH), 56.0 (CH<sub>3</sub>), 55.9 (CH<sub>3</sub>), 55.1 (CH<sub>3</sub>), 44.5 (CH<sub>2</sub>), 37.2 (CH<sub>2</sub>), 31.3 (CH<sub>2</sub>). **IR (neat, v/cm<sup>-1</sup>):** 3375 (w), 2981 (s), 1655 (m), 1602 (m), 1509 (s), 1446 (m), 1252 (s), 1176 (m), 1139 (s), 1080 (m), 1019 (m), 959 (m), 833 (s), 738 (m), 620 (m). **HR-MS (TOF-AP+)** calculated for C<sub>24</sub>H<sub>28</sub>N<sub>3</sub>O<sub>4</sub> 422.2080, found 422.2079.

***N*-(3-(1H-Imidazol-1-yl)propyl)-3,6,7-trimethoxyphenanthrene-9-carboxamide, 16:** In analogy to the preparation of **15**, methyl 3,6,7-trimethoxyphenanthrene-9-carboxylate (**9**, 700 mg, 2.15 mmol) was converted into the target compound **16** (730 mg, 1.74 mmol, 81%) which was obtained as a yellow waxy solid.

**<sup>1</sup>H-NMR (400 MHz, CDCl<sub>3</sub>):** δ/ppm 7.71 (s, 1H), 7.65 (s, 1H), 7.63 (d, *J* = 2.5 Hz, 1H), 7.61 (d, *J* = 8.8 Hz, 1H), 7.50 (s, 1H), 7.49 (s, 1H), 7.10 (dd, *J* = 8.7, 2.4 Hz, 1H), 7.06 (t, *J* = 5.9, 5.9 Hz, 1H), 6.99 (t, *J* = 1.1 Hz, 1H), 6.93 (t, *J* = 1.3 Hz, 1H), 4.03 (s, 3H), 4.01 (t, *J* = 6.8 Hz, 2H), 3.97 (s, 3H), 3.92 (s, 3H), 3.43 (app q, *J* = 6.8 Hz, 2H), 2.07 (p, *J* = 6.8 Hz, 2H). **<sup>13</sup>C-NMR (100 MHz, CDCl<sub>3</sub>):** δ/ppm 170.5 (C), 159.2 (C), 149.6 (C), 149.1 (C), 137.2 (CH), 131.9 (C), 130.7 (CH), 129.4 (CH), 129.1 (C), 124.8 (C), 124.7 (CH), 124.2 (C), 124.1 (C), 118.9 (CH), 115.9 (CH), 106.4 (CH), 103.7 (CH), 103.2 (CH), 55.9 (CH<sub>3</sub>), 55.8 (CH<sub>3</sub>), 55.5 (CH<sub>3</sub>), 44.8 (CH<sub>2</sub>), 37.2 (CH<sub>2</sub>), 31.2 (CH<sub>2</sub>). **IR (neat, v/cm<sup>-1</sup>):** 3259 (broad), 2939 (m), 1618 (m), 1522 (s), 1508 (s), 1473 (s), 1270 (s), 1228 (s), 1206 (s), 1158 (m), 1033 (m), 832 (w), 734 (w). **HR-MS (TOF AP+)** calculated for C<sub>24</sub>H<sub>26</sub>N<sub>3</sub>O<sub>4</sub> 420.1923, found 420.1921.

***(E)*-N-(3-(1H-Imidazol-1-yl)propyl)-2-(3,4-dimethoxyphenyl)-3-(4-methoxyphenyl)prop-2-en-1-amine, 17:** To a solution of *(E)*-N-(3-(1H-imidazol-1-yl)propyl)-2-(3,4-dimethoxyphenyl)-3-(4-methoxyphenyl)acryl-amine (**15**, 500 mg, 1.19 mmol) in dry THF (10 mL, 0.12 M) was added lithium aluminium hydride (LAH, 200 mg, 5.26 mmol) in portions at room temperature. After 2 hours the reaction mixture was carefully quenched by addition of ethyl acetate (1 mL)

and water (3 mL). The resulting emulsion was filtered through a pad of celite (ca. 10 g) and washed with ethyl acetate (30 mL). The resulting pale-yellow solution was evaporated to dryness yielding a yellow oil that was purified by column chromatography (20-40% EtOAc/hexanes). The desired product **17** was obtained as a colorless oil that solidified upon standing (445 mg, 1.09 mmol, 92%).

**<sup>1</sup>H-NMR (400 MHz, CDCl<sub>3</sub>):** δ/ppm 7.40 (s, 1H), 7.33 – 7.29 (m, 2H), 7.06 – 7.03 (m, 2H), 7.02 (s, 1H), 6.92 – 6.86 (m, 3H), 6.82 (s, 1H), 6.77 (s, 1H), 3.96 (t, *J* = 6.9 Hz, 2H), 3.91 (s, 3H), 3.89 (s, 3H), 3.82 (s, 3H), 3.75 (s, 2H), 2.54 (t, *J* = 6.6 Hz, 2H), 1.82 (p, *J* = 6.8 Hz, 2H). **<sup>13</sup>C-NMR (100 MHz, CDCl<sub>3</sub>):** δ/ppm 158.6 (C), 149.0 (C), 148.7 (C), 138.3 (C), 137.2 (CH), 134.5 (C), 130.0 (2CH+C), 129.4 (CH), 129.1 (CH), 118.9 (CH), 118.7 (CH), 113.8 (2CH), 111.2 (CH), 109.9 (CH), 56.0 (2CH<sub>3</sub>), 55.3 (CH<sub>3</sub>), 48.3 (CH<sub>2</sub>), 45.8 (CH<sub>2</sub>), 44.6 (CH<sub>2</sub>), 31.1 (CH<sub>2</sub>). **IR (neat, v/cm<sup>-1</sup>):** 2935 (w), 2836 (w), 1670 (m), 1604 (m), 1509 (s), 1463 (m), 1246 (s), 1176 (m), 1143 (m), 1024 (s), 812 (m), 765 (m), 731 (s), 683 (m), 531 (m). **HR-MS (TOF-AP+)** calculated for C<sub>24</sub>H<sub>30</sub>N<sub>3</sub>O<sub>3</sub> 408.2287, found 408.2285.

**3-(1*H*-Imidazol-1-yl)-*N*-((3,6,7-trimethoxyphenanthren-9-yl)methyl)propan-1-amine, 18:** In analogy to the preparation of compound **17**, *N*-(3-(1*H*-imidazol-1-yl)propyl)-3,6,7-trimethoxyphenanthrene-9-carboxamide (**16**, 500 mg, 1.19 mmol) was converted to the target compound that was isolated as a waxy solid (454 mg, 1.12 mmol, 94%).

**<sup>1</sup>H-NMR (400 MHz, CDCl<sub>3</sub>):** δ/ppm 7.80 (s, 1H), 7.75 (d, *J* = 2.4 Hz, 1H), 7.68 (d, *J* = 8.7 Hz, 1H), 7.40-7.45 (m, 2H), 7.36 (s, 1H), 7.13 (dd, *J* = 8.7, 2.4 Hz, 1H), 6.96 (t, *J* = 1.1 Hz, 1H), 6.78 (t, *J* = 1.1 Hz, 1H), 4.04 (s, 2H), 4.02 (s, 3H), 3.97 (s, 3H), 3.94 (s, 3H), 3.91-3.95 (m, 2H), 2.64 (t, *J* = 6.7 Hz, 2H), 1.87 (app p, *J* = 6.7 Hz, 2H). **<sup>13</sup>C-NMR (100 MHz, CDCl<sub>3</sub>):** δ/ppm 158.1 (C), 149.2 (C), 148.7 (C), 137.1 (CH), 130.8 (C), 130.5 (C), 129.9 (CH), 129.3 (CH), 126.2 (C),

125.7 (C), 124.9 (C), 124.6 (CH), 118.9 (CH), 115.5 (CH), 104.8 (CH), 103.8 (CH), 103.7 (CH), 56.0 (CH<sub>3</sub>), 55.9 (CH<sub>3</sub>), 55.5 (CH<sub>3</sub>), 52.5 (CH<sub>2</sub>), 46.3 (CH<sub>2</sub>), 44.7 (CH<sub>2</sub>), 31.5 (CH<sub>2</sub>). **IR (neat, v/cm<sup>-1</sup>):** 3002 (w), 2935 (w), 2832 (w), 1609 (s), 1523 (s), 1509 (s), 1467 (s), 1269 (s), 1205 (s), 1161 (m), 1070 (m), 1032 (m), 834 (w), 731 (m). **HR-MS (TOF AP+)** calculated for C<sub>24</sub>H<sub>28</sub>N<sub>3</sub>O<sub>3</sub> 406.2131, found 406.2137.

**3,6,7-Trimethoxy-11,12,13,14,14a,15-hexahydro-9H-dibenzo[f,h]pyrido[1,2-b]isoquinolin-15-ol (19a and 19b):** To a solution of 3,6,7-trimethoxy-12,13,14,14a-tetrahydro-9H-dibenzo[f,h]pyrido[1,2-b]isoquinolin-15(11*H*)-one (**13**, 250 mg, 0.64 mmol) in dry THF (10 mL, 0.06 M) was slowly added lithium aluminium hydride (73 mg, 1.92 mmol, 3.0 equiv.). After stirring at room temperature for 1 h the mixture was carefully quenched by addition of ethyl acetate (1 mL) and water (1 mL). Filtration over a pad of celite (ca. 5 g) and elution with ethyl acetate (20 mL) yielded after evaporation the crude mixture of **19a** and **19b** (213 mg, 0.54 mmol, 85%) in a 1:2 ratio as evidenced by <sup>1</sup>H-NMR. The separation of this mixture was accomplished by preparative thin layer chromatography (2 runs) using EtOAc/hexanes (30:70) as solvent system.

**Rac-(14*aR*,15*S*)-3,6,7-Trimethoxy-11,12,13,14,14*a*,16-hexahydro-9H-dibenzo[*f,h*]pyrido-[1,2-*b*]isoquinolin-15-ol, 19a:**

**<sup>1</sup>H-NMR (700 MHz, CDCl<sub>3</sub>):** δ/ppm 8.30 (d, *J* = 9.1 Hz, 1H), 7.82 (d, *J* = 2.6 Hz, 1H), 7.80 (s, 1H), 7.21 (dd, *J* = 9.1, 2.5 Hz, 1H), 6.69 (s, 1H), 4.99 (d, *J* = 5.6 Hz, 1H), 4.10 (s, 3H), 4.01 (s, 3H), 3.93 (d, *J* = 15.0 Hz, 1H), 3.89 (s, 3H), 3.03 (br s, 1H), 2.44 (br s, 2H), 2.10 (s, 1H), 1.83 (d, *J* = 12.7 Hz, 1H), 1.75 (d, *J* = 14.3 Hz, 1H), 1.64 (d, *J* = 13.8 Hz, 1H), 1.41 (q, *J* = 12.7 Hz, 1H). 3 Resonances were not observed due to broadening effects. **<sup>13</sup>C-NMR (176 MHz, CDCl<sub>3</sub>):** δ/ppm 157.7 (C), 149.4 (C), 148.9 (C), 131.1 (C), 127.5 (CH), 124.1 (C), 124.0 (C), 123.8 (C), 114.8 (CH), 104.6 (CH), 103.7 (CH), 103.2 (CH), 70.3 (CH), 65.5 (CH), 55.9 (CH<sub>3</sub>), 55.8 (CH<sub>3</sub>), 55.5 (CH<sub>3</sub>), 54.5 (CH<sub>2</sub>), 23.3 (CH<sub>2</sub>). 5 Resonances

were not observed (2 C, 3 CH<sub>2</sub>). **IR (neat, v/cm<sup>-1</sup>):** 3300 (broad), 2936 (m), 1732 (w), 1615 (m), 1514 (s), 1471 (s), 1426 (m), 1262 (s), 1235 (m), 1206 (s), 1172 (m), 1147 (m), 1039 (s), 914 (m), 840 (m), 731 (m). **HR-MS (ESI-TOF+)** calculated for C<sub>24</sub>H<sub>28</sub>NO<sub>4</sub> 394.2018, found 394.2028.

**Rac-(14*aR*,15*R*)-3,6,7-Trimethoxy-11,12,13,14,14*a*,16-hexahydro-9*H*-dibenzo[*f,h*]pyrido-[1,2-*b*]isoquinolin-15-ol, 19b:**

**<sup>1</sup>H-NMR (600 MHz, CDCl<sub>3</sub>):** δ/ppm 8.35 (d, *J* = 9.0 Hz, 1H), 7.68 (d, *J* = 2.6 Hz, 1H), 7.50 (s, 1H), 7.21 (dd, *J* = 9.0, 2.5 Hz, 1H), 5.91 (s, 1H), 4.59 (d, *J* = 2.5 Hz, 1H), 4.07 (s, 3H), 4.02 (s, 3H), 3.71 (s, 3H), 2.84-3.00 (m, 2H), 2.80 (d, *J* = 14.9 Hz, 1H), 2.24 (qd, *J* = 13.3, 3.8 Hz, 1H), 2.07 (d, *J* = 11.2 Hz, 1H), 1.90-2.00 (m, 2H), 1.82 (q, *J* = 13.1 Hz, 1H), 1.73 (d, *J* = 13.1, Hz, 1H), 1.67 (d, *J* = 12.2 Hz, 1H), 1.27-1.35 (m, 1H). **<sup>13</sup>C-NMR (151 MHz, CDCl<sub>3</sub>):** δ/ppm 157.4 (C), 148.5 (C), 148.3 (C), 130.4 (C), 127.8 (C), 126.8 (CH), 124.7 (C), 124.0 (C), 123.5 (2C), 111.4 (CH), 104.0 (CH), 102.9 (CH), 102.5 (CH), 66.5 (CH), 62.5 (CH), 56.7 (CH<sub>2</sub>), 55.6 (CH<sub>3</sub>), 55.4 (CH<sub>3</sub>), 55.3 (CH<sub>3</sub>), 55.2 (CH<sub>2</sub>), 27.0 (CH<sub>2</sub>), 25.1 (CH<sub>2</sub>), 24.1 (CH<sub>2</sub>). **IR (neat, v/cm<sup>-1</sup>):** 3184 (broad), 2938 (m), 1743 (w), 1611 (m), 1534 (m), 1511 (s), 1470 (s), 1424 (m), 1257 (s), 1204 (s), 1171 (s), 1127 (m), 1042 (s), 910 (m), 839 (m), 730 (s). **HR-MS (ESI-AP+)** calculated for C<sub>24</sub>H<sub>28</sub>NO<sub>4</sub> 394.2018, found 394.1990. **X-ray analysis: xxxx**

#### 4.1. Biological Evaluation

##### 4.2.1. Cells culture

Hepatocellular carcinoma cell lines (Huh7, FOCUS, Hep3B, HepG2 and Mahlavu), human breast carcinoma cells (MCF7) and human colon carcinoma cells (HCT116) were grown in Dulbecco's Modified Eagles Medium (DMEM) supplemented with 10% fetal bovine serum (GIBCO, Invitrogen), 1% non-essential amino acids (GIBCO, Invitrogen) and SNU-475 were grown in RPMI-1640 media (Invitrogen GIBCO) supplemented with 10% FBS, 2 mM L-glutamine. All media contained 100 units/ml penicillin and streptomycin and cells were maintained at 37 °C in a humidified incubator under 5% CO<sub>2</sub>.

#### *4.2.2. NCI-60 Sulforhodamine B Assay*

Cells were plated in 96-well plates (HCT116 – 3000, Huh7, Hep3B, HepG2, MCF-7 –2000, Mahlavu, FOCUS, SNU475-1000 cells per well) and grown for 24 hours in an incubator. The compounds were dissolved in DMSO and were prepared 20mM stock solution. The compounds were tested starting from 40  $\mu$ M to 2,5  $\mu$ M in triplicates. The compounds, which were below 2,5  $\mu$ M, were tested starting from 2,5  $\mu$ M to 0,03  $\mu$ M. After 72h of incubation, cells were fixed using 10% (v/v) trichloroacetic acid (MERCK) for an hour. The fixed plates were dried and samples were stained with sulforhodamine B (SRB) solution (50  $\mu$ l of a 0.4% (m/v) of SRB in 1% acetic acid solution) for 10 min. The excess amount of SRB dye was discarded by washing samples with 1% acetic acid and left for air-drying. The protein bound SRB dye was dissolved in 10 mM Tris-base and its absorbance was measured with 96-well plate reader at 515 nm. The IC<sub>50</sub> values were calculated based on DMSO control normalization.

#### *4.2.3. Real-time cell growth surveillance by electronic sensing (RT-CES)*

Real-time cell growth analysis was performed using the the xCELLigence System (Roche Applied Sciences). The Huh7 (2000) and Mahlavu (1000) cells were plated in 96 well E plates. In proliferation step, the cellular growth was analyzed with cell index measurements in 30 min intervals. After 24 h of incubation, when cells reach the log growth phase, they were treated with Boehmeriasin derivatives compounds starting from 1  $\mu$ M and 2 folds serial diluted 4 times. The cell index values (CI) were initially monitored every 10 min for 24 h and then CI were recorded in 30 min intervals. After 72 h of incubation, the cellular growth inhibition was calculated based on the DMSO normalization.

#### *4.2.4 DCFH-DA Staining for ROS detection*

Huh7 cells were plated into 6 well plates and treated with 1  $\mu$ M Boehmeriasin derivatives. After treatment, samples were washed with PBS 3 times, they were incubated with DCFH-DA assay solution for 15 min in humidified chamber at 37 °C. The solution was aspirated and cells were washed with PBS 2 times. The staining was analyzed with fluorescence microscope.

#### *4.2.5. Western Blot Analysis*

Huh7 and Mahlavu cells were treated with the Boehmeriasin derivatives compounds (IC<sub>100</sub> concentrations) or with DMSO control for 48 hours. After incubation period, the cells were collected with scraper, their total proteins were isolated and protein concentrations were calculated with Bradford assay. 20-50 µg from all proteins were loaded to Bis-Tris gel and western blot was performed with Novex® NuPAGE® Bis-Tris Electrophoresis system. Then the proteins were transferred to nitrocellulose membrane via XCell IITM Blot Module. Cyclin-B1 (554177, BD), Cdc2/Cdk1 (PC25, Calbiochem), PARP (9532, Cell Signaling), Cyclin E (CC05, Calbiochem), Cdk2 (sc6248, Santa Cruz), phosphor ASK1 (3765, Cell Signaling), phosphor SAPK/JNK (9251, Cell Signaling), phosphor AKT (9275, Cell Signaling) and AKT (9272, Cell Signaling) antibodies were used in 1:100 to 1:500 5% BSA-TBS-T. β-actin (#A5441, Sigma) and Calnexin (C4731, Sigma) antibodies were used in 1:1000 concentration for equal loading.

#### *4.2.6. Immunofluorescence Assay*

Huh7 and Mahlavu cells were seeded in 6 well plates on coverslips. After 24 hours, cells were treated with the 1 µM Boehmeriasin derivatives for 72 hours. Camptothecin was used as positive control for cytochrome c activity. DMSO control were given to cells in the same amount of the compounds. After the incubation period, cells were fixed with ice-cold methanol for 15 min. The cytochrome c primary antibody (Santa Cruz, 1:100 in 0,1 % TBS-Tween) were applied for 1 hour. FITC conjugated secondary antibody (Santa Cruz, 1:200 in 0,1 % TBS-Tween) were applied for 1 hour. The cells were mounted with UltraCruz DAPI mounting medium and photos were taken with fluorescence microscopy.

#### *4.2.7. Flow Cytometry for Cell Cycle Analysis*

Huh7 and Mahlavu cells were seeded onto 100 mm culture dishes. After 24 h, cells were treated with the 1 µM Boehmeriasin derivatives. After 24 h, 48 h and 72 h of incubation, cells were fixed with ice-cold 70% ethanol for 3 hours at -20 °C. Cell cycle analysis was carried out by PI (Propidium Iodide) staining using MUSE Cell Analyzer according to the manufacturer's recommendations (Millipore).

## AUTHOR INFORMATION

### Corresponding Authors

\* [marcus.baumann@ucd.ie](mailto:marcus.baumann@ucd.ie) (Marcus Baumann); [rengul@metu.edu.tr](mailto:rengul@metu.edu.tr) (Rengul Cetin-Atalay)

### Author Contributions

The manuscript was written through contributions of all authors. All authors have given approval to the final version of the manuscript.

## ACKNOWLEDGMENT

We gratefully acknowledge funding from the Royal Society (to MB and IRB), the British Council for a travel grant (to MB) and Turkish Ministry of Development Kansil\_2016K121540 project (to RA and EA). Finally, we are thankful to Dr Andrei Batsanov (University of Durham) for solving the X-ray structure of compound **19b**.

## ABBREVIATIONS

CCR2, CC chemokine receptor 2; CCL2, CC chemokine ligand 2; CCR5, CC chemokine receptor 5; **PARP, xxx**; CDI, carbonyl diimidazole; TLC, thin layer chromatography; LAH, lithium aluminium hydride

## REFERENCES

- (1) Ferlay, J.; Soerjomataram, I.; Dikshit, R.; Eser, S.; Mathers, C.; Rebelo, M.; Parkin, D.M.; Forman, D.; Bray, F. Cancer incidence and mortality worldwide: sources, methods and major patterns in GLOBOCAN 2012. *Int. J. Cancer* **2015**, *136*, E359-E386.
- (2) El-Serag H.B. Hepatocellular carcinoma. *N. Engl. J. Med.* **2011**, *365*, 1118–1127.
- (3) Bosch F.X.; Ribes J.; Cleries R.; Diaz M. Epidemiology of hepatocellular carcinoma. *Clin. Liver Dis.* **2005**, *9*, 191–211.
- (4) El-Serag H.B.; Rudolph K.L. Hepatocellular carcinoma: epidemiology and molecular carcinogenesis. *Gastroenterology* **2007**, *132*, 2557–2576.
- (5) Sherif Z.A.; Saeed A.; Ghavimi S.; Nouraiie S.M.; Laiyemo A.O.; Brim H.; Ashktorab H. Global Epidemiology of Non-alcoholic Fatty Liver Disease and Perspectives on US Minority Populations. *Dig. Dis. Sci.* **2016**, *61*, 1214-1225.
- (6) Farazi P.A.; DePinho R.A. Hepatocellular carcinoma pathogenesis: from genes to environment. *Nat. Rev. Cancer* **2006**, *6*, 674-687.
- (7) Hertl M.; Cosimi A.B. Liver transplantation for malignancy. *Oncologist* **2005**, *10*, 269-281.
- (8) Llovet J.M.; Ricci S.; Mazzaferro V.; Hilgard P.; Gane E.; Blanc J.F.; de Oliveira A.C.; Santoro A.; Raoul J.L.; Forner A.; Schwartz M.; Porta C. Zeuzem S.; Bolondi L.; Greten T.F.; Galle P.R.; Seitz J.F.; Borbath I.; Häussinger D.; Giannaris T.; Shan M.; Moscovici M.; Voliotis D.; Bruix J. Sorafenib in advanced hepatocellular carcinoma. *N. Engl. J. Med.* **2008**, *359*, 378-390.

- (9) Brui, J.; Qin, S.; Merle, P.; Granito, A.; Huang, Y.-H.; Bodoky, G.; Pracht, M.; Yokosuka, O.; Rosmorduc, O.; Breder, V.; Gerolami, R.; Masi, G.; Ross, P.J.; Song, T.; Bronowicki, J.-P.; Ollivier-Hourmand, I.; Kudo, M.; Cheng, A.-L.; Llovet, J.M.; Finn, R.S.; LeBerre, M.-A.; Baumhauer, A.; Meinhardt, G.; Han, G. Regorafenib for patients with hepatocellular carcinoma who progressed on sorafenib treatment (RESORCE): a randomised, double-blind, placebo-controlled, phase 3 trial. *Lancet* **2017**, *389*, 56-66.
- (10) Richard S.; Finn P.; Merle A.; Granito A.; Jordi B. Outcomes with sorafenib (SOR) followed by regorafenib (REG) or placebo (PBO) for hepatocellular carcinoma (HCC): Results of the international, randomized phase 3 RESORCE trial. *Journal of Clinical Oncology* **2017**, *35* (4\_suppl), 344.
- (11) Luo, Y.; Liu, Y.; Luo, D.; Gao, X.; Li, B.; Zhang, G. Cytotoxic alkaloids from *Boehmeria siamensis*. *Planta Med.* **2003**, *69*, 842-845.
- (12) Cui, M.; Wang, Q.; Total synthesis of phenanthrol-quinolizidine alkaloids: ( $\pm$ )-cryptopleurine, ( $\pm$ )-boehmeriasin A, ( $\pm$ )-boehmeriasin B and ( $\pm$ )-hydroxycryptopleurine. *Eur. J. Org. Chem.* **2009**, *31*, 5445-5451.
- (13) Wei, H.; Yan, J.; Liu, J.; Luo, D.; Zhang, G. Induction of G1 arrest and differentiation in MDA-MB-231 breast cancer cells by boehmeriasin A, a novel compound from plant. *Int. J. Gynecol. Cancer* **2006**, *16*, 165-170.
- (14) Chemler, S.R. Phenanthroindolizidines and Phenanthroquinolizidines: Promising Alkaloids for Anti-Cancer Therapy. *Curr. Bioact. Comp.* **2009**, *5*, 2-19.

- (15) Saraswati, S.; Kanaujia, P.K.; Kumar, S.; Kumar, R.; Alhaider, A.A. Tylophorine, a phenanthraindolizidine alkaloid isolated from *Tylophora indica* exerts antiangiogenic and antitumor activity by targeting vascular endothelial growth factor receptor 2-mediated angiogenesis. *Mol. Cancer* **2013**, *12*, 82.
- (16) Yang, C.-W.; Lee, Y.-Z.; Hsu, H.-Y.; Wu, C.-M.; Chang, H.-Y.; Chao, Y.-S.; Lee, S.-J. c-Jun-mediated anticancer mechanisms of tylophorine. *Carcinogenesis* **2013**, *34*, 1304-1314.
- (17) Kim, E.-H.; Min, H.-Y.; Chung, H.-J.; Song, J.; Park, H.-J.; Kim, S.; Lee, S.K. Anti-proliferative activity and suppression of P-glycoprotein by (–)-antofine, a natural phenanthroindolizidine alkaloid, in paclitaxel-resistant human lung cancer cells. *Food Chem. Toxicology* **2012**, *50*, 1060-1065.
- (18) Fu, Y.; Lee, S.K.; Min, H.-Y.; Lee, T.; Lee, J.; Cheng, M.; Kim, S. Synthesis and structure-activity studies of antofine analogues as potential anticancer agents. *Bioorg. Med. Chem. Lett.* **2007**, *17*, 97-100.
- (19) Kwon, Y.; Song, J.; Lee, H.; Kim, E.-Y.; Lee, K.; Lee, S.K.; Kim, S. Design, Synthesis, and Biological Activity of Sulfonamide Analogues of Antofine and Cryptopleurine as Potent and Orally Active Antitumor Agents. *J. Med. Chem.* **2015**, *58*, 7749-7762.
- (20) Antofine and cryptopleurine derivatives as anticancer agents. US Patent US20120283220A1 (published Nov 8, 2012).

- (21) Jin, H.R.; Jin, S.Z.; Cai, X.F.; Li, D.; Wu, X.; Nan, J.X.; Lee, J.J.; Jin, X. Cryptopleurine Targets NF- $\kappa$ B-Pathway, Leading to Inhibition of Gene Products Associated with Cell Survival, Proliferation, Invasion, and Angiogenesis. *PloS ONE* **2012**, *7*, e40355.
- (22) Zing, W.; Herndon, J.W. Total Synthesis of (+)-Antofine and (-)-Cryptopleurine. *Eur. J. Org. Chem.* **2013**, 3112-3122.
- (23) Fürstner, A.; Kennedy, J.W.J. Total Syntheses of the Tylophora Alkaloids Cryptopleurine, (-)-Antofine, (-)-Tylophorine, and (-)-Ficuseptine C. *Chem. Eur. J.* **2006**, *12*, 7398-7410.
- (24) Christodoulou, M.S.; Calogero, F.; Baumann, M.; Garcia-Argaez, A.N.; Pieraccini, S.; Sironi, M.; Dapiaggi, F.; Bucci, R.; Brogгинi, G.; Gazzola, S.; Liekens, S.; Silvani, A.; Lahtela-Kakkonen, M.; Martinet, N.; Nonell-Canals, A.; Santamaria-Navarro, E.; Baxendale, I.R.; Dalla Via, L.; Passarella, D. Boehmeriasin A as new lead compound for the inhibition of topoisomerases and SIRT2. *Eur. J. Med. Chem.* **2015**, *92*, 766-775
- (25) Durmaz I.; Guven E.B.; Ersahin T.; Ozturk M.; Calis I.; Cetin-Atalay R. Liver cancer cells are sensitive to Lanatoside C induced cell death independent of their PTEN status. *Phytomedicine* **2016**, *23*, 42-51.
- (26) Irmak M.B.; Ince G.; Ozturk M.; Cetin-Atalay R.; Acquired tolerance of hepatocellular carcinoma cells to selenium deficiency: a selective survival mechanism? *Cancer Res.* **2003**, *63*, 6707-6715.